HHS Public Access

Author manuscript

Conf Proc IEEE Eng Med Biol Soc. Author manuscript; available in PMC 2017 August 08.

Published in final edited form as:

Conf Proc IEEE Eng Med Biol Soc. 2015 August ; 2015: 3783–3786. doi:10.1109/EMBC.2015.7319217.

Atrial Sources Identification by Causality Analysis during Atrial Fibrillation

Miguel Rodrigo [Student member, IEEE],
BIO-ITACA at Universitat Politécnica de Valencia, Valencia, Spain

Andreu M. Climent,
Cardiology Department, Hospital General Universitario Gregorio Marañón, Madrid, Spain

Alejandro Liberos,
BIO-ITACA at Universitat Politécnica de Valencia, Valencia, Spain

Francisco Fernández-Avilés,
Cardiology Department, Hospital General Universitario Gregorio Marañón, Madrid, Spain

Omer Berenfeld,
Center for Arrhythmia Research, University of Michigan, Ann Arbor, USA

Felipe Atienza, and
Cardiology Department, Hospital General Universitario Gregorio Marañón, Madrid, Spain

María S. Guillem
BIO-ITACA at Universitat Politécnica de Valencia, Valencia, Spain

Abstract

Ablation of electrical drivers during atrial fibrillation (AF) has been proved as an effective therapy to prevent recurrence of fibrillatory episodes. This study presents a new methodology based on causality analysis that is able to identify the hierarchical dominance of atrial areas driving AF.

Realistic mathematical models of the atrial electrical activity during AF were used to assess the validity of our method. Identification of the dominant atrial propagation patterns was achieved by computing causal relations between multiple electrogram signals. The causal relationships between atrial areas during the fibrillatory processes were summarized into a recurrence map, highlighting the hierarchy and dominant areas.

Recurrence maps computed from causality analysis allowed the identification of sites responsible for maintenance of the arrhythmia. These maps were able to locate the position of the atrial driver in fibrillatory processes with a single rotor, with 2 rotors or with several drivers. Additionally, the correspondence between the nodal values of the recurrence map and the distance to the rotor core has been established.

Causal analysis consistently estimated propagation patterns and location of atrial drivers during AF. This methodology could guide ablation procedures in AF patients.

Phone: +34-963-877-968; mirodbor@teleco.upv.es.

I. Introduction

Atrial fibrillation (AF) can be driven by atrial areas responsible for the maintenance of the arrhythmia [1–3], and ablation of these dominant areas can prevent the arrhythmia recurrence [4]. Atrial drivers can be located everywhere in the atria [5], so their identification in each patient is a goal for the ablation therapy. Although there are some methods for locating these atrial sources [6–7], like the detection of the regions with highest dominant frequencies (DF), their efficiency remain elusive.

This work proposes a novel tool for dominant areas location based on the search for the strongest cause-effect relationships between multiple electrograms that allows locating the electrical sources driving AF. This analysis can be used to estimate the dominant propagation pattern and to locate the region that predominantly acts as a source of electrical activations. As a first approach and due to the difficulty in obtaining simultaneous recordings of the electrical activity across the whole atria, we have used here mathematical models of the atrial electrical activity during fibrillatory processes to assess the validity of our method.

II. Methods

A. Mathematical models of the atrial electrical activity

A realistic 3D anatomical model of both atria was used to simulate the atrial electrical activity during fibrillatory processes (285,780 nodes and 566,549 triangular patches) [8]. A gradient of the electrophysiological properties ($I_{k,ACH}$) of the atrial myocardium was introduced into the mathematical model in order to obtain realistic propagation patterns with different activation rates. The reaction-diffusion system with the Courtemanche cell model kinetics [9–10] was solved by using the Runge-Kutta integration method with an adaptive temporal step on a graphic processors unit (NVIDIA Tesla C2075 6G) [11].

From each computational simulation, a uniform mesh of pseudo-unipolar electrograms was calculated under the assumption of a homogenous, unbounded and quasi-static medium by using the following expression:

$$V_{\vec{r}} = \sum_{\vec{r}} \left(\frac{\vec{r}}{r^3} \right) \cdot \vec{\nabla} V_m \quad (1)$$

where r is the distance vector between the measuring point and a point in the tissue domain, ∇ denotes the gradient operator and V_m is the transmembrane potential distribution. Computed electrograms were stored for further processing at a sampling frequency of 1 kHz.

B. Causality Analysis Method

Causal relations were searched between N simultaneous neighboring signals, which were divided into K_n overlapping time segments of length equal to the inverse of the DF. Under the assumption that a given observation $x_i(t)$ can result from previous observations in

neighboring nodes $x_j(t-\tau)$, their cause-effect relationship level can be assessed by a univariate autoregressive model (ARM):

$$x_i(t)=\sum_{\tau=t_{\min}}^{t_{\max}} \alpha_\tau \cdot x_j(t-\tau)+\varepsilon_{\mathrm{ij}}(t) \quad (2)$$

where α_τ are the ARM coefficients and $\varepsilon_{ij}(t)$ is the error in the prediction of x_i from x_j by using the ARM, which can be assumed to be a white noise process characterized by its variance $\sigma^2_{\varepsilon ij}$. The order of the ARM model is given by $t_{max}-t_{min}$, where $t_{min}=d/v_{max}$, $t_{max}=d/v_{min}$, d is the distance between electrodes, and v_{max} and v_{min} are the maximum and minimum conduction velocities respectively. ARM coefficients are estimated by using the least-squares method [12].

In order to compare the degree of causality between signals with inherent differences in their variance, we use a statistical approach based on influence measure. This measure compares the variance measured by applying the ARM model with source and destiny signals $\sigma^2_{\varepsilon ij}$ with the variance value $\sigma^2_{\varepsilon ii}$ obtained by applying the model on the destiny signal itself. We defined the Influence Ratio matrix (IR, (3)), computed for a given pair of signals (i,j), as the ratio between variances of the error of ARM models for the source signal ($\sigma^2_{\varepsilon ij}$) and for itself ($\sigma^2_{\varepsilon ii}$):

$$\mathrm{IR}_{\mathrm{ij}}=\frac{\sigma^2_{\varepsilon_{\mathrm{ii}}}}{\sigma^2_{\varepsilon_{\mathrm{ij}}}} \quad ; \quad \mathrm{IRN}_{\mathrm{ij}}=\frac{\frac{1}{K_n}\sum_{k=1}^{K_n}\mathrm{IR}_{\mathrm{ij},k}}{\frac{1}{K_n}\sum_{k=1}^{K_n}\sum_{i=1}^{N}\mathrm{IR}_{\mathrm{ij},k}} \quad (3,4)$$

The IR is measured for all the K_n overlapping intervals ($IR_{ij,k}$) and the influence of a signal x_j in a signal x_i is summarized by normalizing the IR matrix (IRN, (4)), where K_n is the number of signal segments under evaluation.

The Recurrence Map (RM) is then constructed by assigning a value between 0 and 1 to each node according to its probability of behaving as a signal source. These probability values (P) are computed by using the following expression:

$$P=M^{\infty}\times P^{0};M^{\beta}=M^{\beta-1}\times M^{\beta-1};M^{0}=\mathrm{IRN} \quad (5)$$

where M^{∞} is the permanent regime value of IRN matrix and P^0 is the initial probability distribution where $P^0=1/N$. M^{∞} is reached when the value of $\xi = var(P^{\beta} - P^{\beta-1})$ reaches an upper threshold (10^{-10}).

III. Results

With the purpose of demonstrating that atrial drivers during AF can be identified by our causality method we used mathematical models of the atrial electrical activity with three different activation patterns; (i) a functional rotor at the left atrial roof and without a LA- to-RA DF gradient (Fig. 1); (ii) a functional double rotor in 8-figure at the free wall of the right

atrium with RA-to-LA DF gradient (Fig. 2); and (iii) a complex pattern with several drivers: two functional reentries at the left atrial roof, two functional reentries at RA and an anatomical reentry around the RIPV (Fig. 3).

In the first mathematical simulation the fibrillatory process is maintained by a rotor placed on the left atrial roof (Fig. 1A), with a uniform activation frequency in both atria (12 Hz), and no DF gradient (Fig. 1B). The RM (Fig. 1C) depicts the results of the causal methodology on this model. It can be observed that the RM values reach 1 at the vicinity of the rotor, marking the position of the atrial driver. At the rest of the tissue the RM values remain close to 0 showing that there is no other atrial source different to the LA rotor.

In Fig. 2A the propagation pattern from a simulation in which the fibrillatory process is maintained by two counter-rotating rotors at the free wall of the RA is shown. In this case there is a RA-to-LA DF gradient (12 Hz RA, 6 Hz LA, Fig. 2B),and the RA, where the rotors are located, is the fastest. The RM (Fig. 2C) shows the highest values at the free wall of the RA, where the rotors were located. Please note that in this case the area with highest RM values is wider than in the previous case, where there was only a single driver rotor.

Fig. 3A shows the transmembrane potential from a simulation with several drivers. In this case, the AF was maintained by 4 functional reentries (2 at the left atrial roof and 2 at the RA) and by an anatomical reentry around the RIPV. In this case there is no DF gradient: both atria were activated at the same frequency (12 Hz, Fig. 3B). The RM (Fig. 3C) exhibits several areas with values markedly larger than zero, all of them at positions of the atrial drivers: one at the RA and another at the left atrial roof that also extends around the RIPV. In this case, the RM values of the left atrial roof are higher (1) than the RM values at the RA (0.6).

In order to evaluate the spatial profile of AF sources, the RM nodal values obtained at the different atrial models where plotted against the distance to the source with the highest RM value. Fig. 4A shows the RM nodal values from the first model (maintained by a rotor in the LA roof) in comparison with the distance of those nodes to the rotor core. It can be shown as the closest nodes to the rotor core present higher values of the RM than those nodes placed away from the rotor. The RM values can be represented by an exponential decay function from the distance to the rotor core with relatively high accuracy (R^2=0.82). In Fig. 4B the same analysis for the model with two rotors in the RA can be shown. In this case the higher values of the RM are also in the vicinity of the rotors and present an exponential decay with the distance to the atrial driver. The decay curve presents a less steep decay and worse fitting (R^2=0.64), due to the presence of 2 rotors (the distance was obtained to the core of one of them) and the wider extension of the dominant area. Finally, Fig. 4C depicts the RM nodal values of the simulation maintained by multiple drivers. Here we can find 2 areas with high RM nodal values, corresponding to the 2 dominant regions in this model: the left atrial roof and the RA. Consequently, the fitted curve presents an adjusted coefficient (R^2=0.49) lower than the previous models.

IV. Discussion

Several clinical studies provide evidence supporting the existence of localized sources responsible for the maintenance of AF [1–5]. These atrial sources have been postulated to be a consequence of either ectopic activity [1–2], micro-reentries or rotors [3] and can be considered as the center of a hierarchical process in the fibrillatory activity. These hierarchical fibrillatory processes can be identified by their electrical activation pattern whereby the region activated at the highest rate and emitting outward waves is the dominant area. In this work we present a novel technique to analyze the electrical activation patterns to find such dominant regions.

The identification of fibrillatory drivers remains a challenging task due to the irregular wave electrical activity during AF. Isochronal and phase maps of cardiac activation are now quite commonly used to study arrhythmia mechanisms and to guide ablative therapies [3, 7]. However, the construction of isochronal and instantaneous phase maps consider of a short time interval for evaluation (i.e. a single activation cycle), which could be non-typical and could lead to maps that depend on the time interval analyzed and give information about the activity only in that time interval. The causal method reduces such limitation, since it summarizes the electrical activity during a longer time interval (i.e. cumulative activations) into a dominant propagation pattern that depicts the electrical activity in the analyzed interval [13].

The identification of the atrial drivers has also been extensively carried out by the dominant frequency (DF) analysis, since the regions higher activation rates are linked with the presence of atrial drivers [6]. However, in the absence of a left-to-right gradient the results of this approach were poor. Here, we demonstrate that in the presence of a DF gradient in the atria, both DF and causality analysis offer similar results. Nevertheless, the proposed method may allow detecting the origin of activations even in absence of DF gradients.

Identification of causal relationships during irregular activations requires a multipole catheter, with as many recording electrodes as possible. However, balloon (noncontact) or basket multi-electrodes are expensive, complex and not readily available. The presented analysis method could also be carried out by sequentially mapping the atria with a multipolar catheter, avoiding the need for the balloon or basket catheters. However, a study using real recordings of animal or human AF will be necessary to validate the usefulness of our methodology.

V. Conclusion

This work presented a novel methodology for the identification of the atrial sites which are responsible of AF maintenance. Recurrence maps highlight the top-hierarch of dominant regions in the atria and estimate the corresponding propagation pattern, independently of the spatial distribution of DF. The presented methodology is proposed to be useful for guiding ablation procedures in AF patients.

Acknowledgments

Supported in part by: Universitat Politècnica de València through its research initiative program; Generalitat Valenciana Grants (ACIF/2013/021); the Spanish Health Research Fund (PI13/00903 and PI14/00857); Spanish Society of Cardiology; Ministerio de Ciencia e Innovación (Red RIC) and the Centro Nacional de Investigaciones Cardiovasculares (CNIC-13).

References

1. Atienza F, Martins RP, Jalife J. Translational research in atrial fibrillation: a quest for mechanistically based diagnosis and therapy. Circ Arrhythm Electrophysiol. 2012; 5:1207–15. [PubMed: 23022707]
2. Atienza F, et al. RADAR-AF Investigators. Comparison of radiofrequency catheter ablation of drivers and circumferential pulmonary vein isolation in atrial fibrillation: a noninferiority randomized multicenter RADAR-AF trial. J Am Coll Cardiol. 2014; 64:2455–67. [PubMed: 25500229]
3. Narayan SM, et al. Direct Or Coincidental Elimination of Stable Rotors or Focal Sources May Explain Successful Atrial Fibrillation Ablation: On-Treatment Analysis of the CONFIRM (CONventional ablation for AF with or without Focal Impulse and Rotor Modulation) Trial. J Am Coll Cardiol. 2013; 62:137–147.
4. Di Biase L, et al. Atrial fibrillation ablation strategies for paroxysmal patients: randomized comparison between different techniques. Circ Arrhythm electrophysiol. 2009; 2:113–119. [PubMed: 19808455]
5. Hsu LF, et al. Atrial fibrillation originating from persistent left superior vena cava. Circulation. 2004; 109:828–832. [PubMed: 14757689]
6. Atienza F, et al. Real-time dominant frequency mapping and ablation of dominant frequency sites in atrial fibrillation with left-to-right frequency gradients predicts long-term maintenance of sinus rhythm. Heart Rhythm. 2009; 6:33–40. [PubMed: 19121797]
7. Ideker RE, Rogers JM. Human ventricular fibrillation: wandering wavelets, mother rotors, or both? Circulation. 2006; 114:530–532. [PubMed: 16894047]
8. Harrild D, Henriquez CA. Computer model of normal conduction in the human atria. Circ Res. 2000; 87:E25–36. [PubMed: 11009627]
9. Courtemanche M, Ramirez RJ, Nattel S. Ionic mechanisms underlying human atrial action potential properties: insights from a mathematical model. Am J Physiol. 1998; 275:H301–321. [PubMed: 9688927]
10. Kneller J, Ramirez RJ, Chartier D, Courtemanche M, Nattel S. Time-dependent transients in an ionically based mathematical model of the canine atrial action potential. Am J Physiol Heart Circ Physiol. 2002; 282:H1437–1451. [PubMed: 11893581]
11. García VM, et al. Adaptive step ODE algorithms for the 3D simulation of electric heart activity with graphics processing units. Comput Biol Med. 2014; 44:15–26. [PubMed: 24377685]
12. Richter U, et al. A novel approach to propagation pattern analysis in intracardiac atrial fibrillation signals. Ann Biomed Eng. 2011; 39:310–323. [PubMed: 20803171]
13. Berenfeld O, et al. Frequency dependent breakdown of wave propagation into fibrillatory conduction across the pectinate muscle network in the isolated sheep right atrium. Circ. Res. 2002; 90:1173–1180. [PubMed: 12065320]

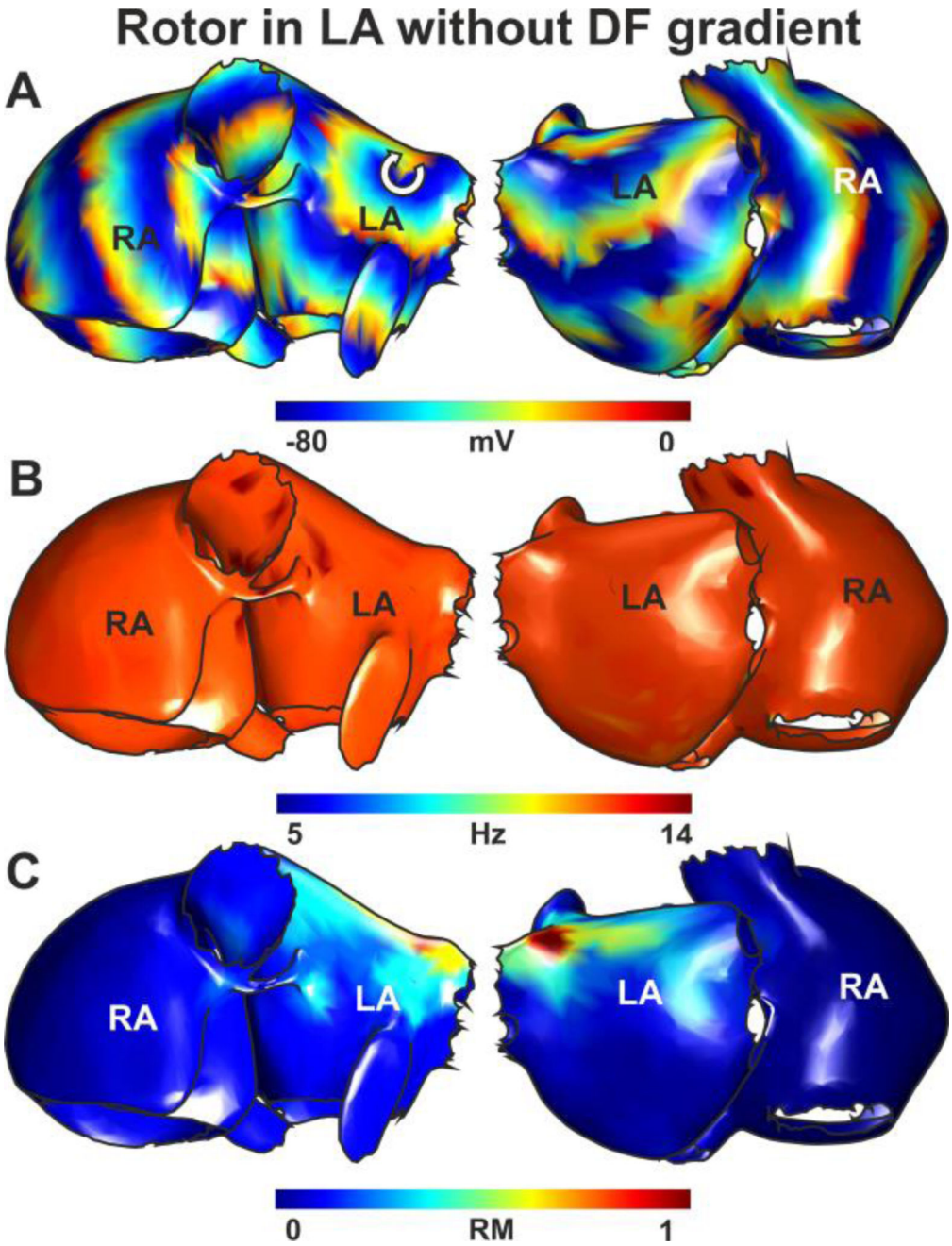

Figure 1.
Anterior and posterior views of atrial model with a rotor in LA without DF gradient. (A) Transmembrane potentials. (B) DF map. (C) Recurrence map.

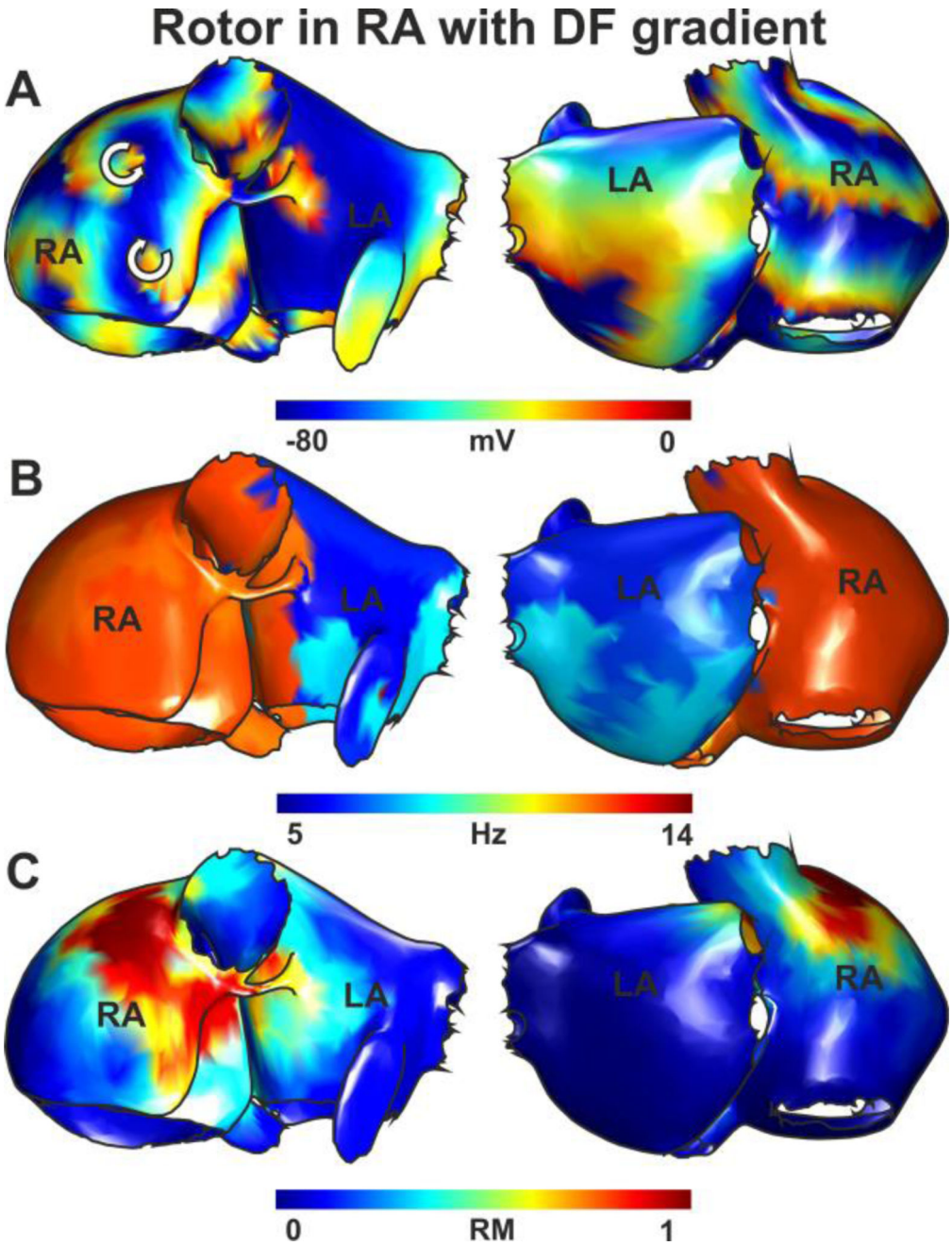

Figure 2.
Anterior and posterior views of atrial model with a rotor in RA with DF gradient. (A) Transmembrane potentials. (B) DF map. (C) Recurrence map.

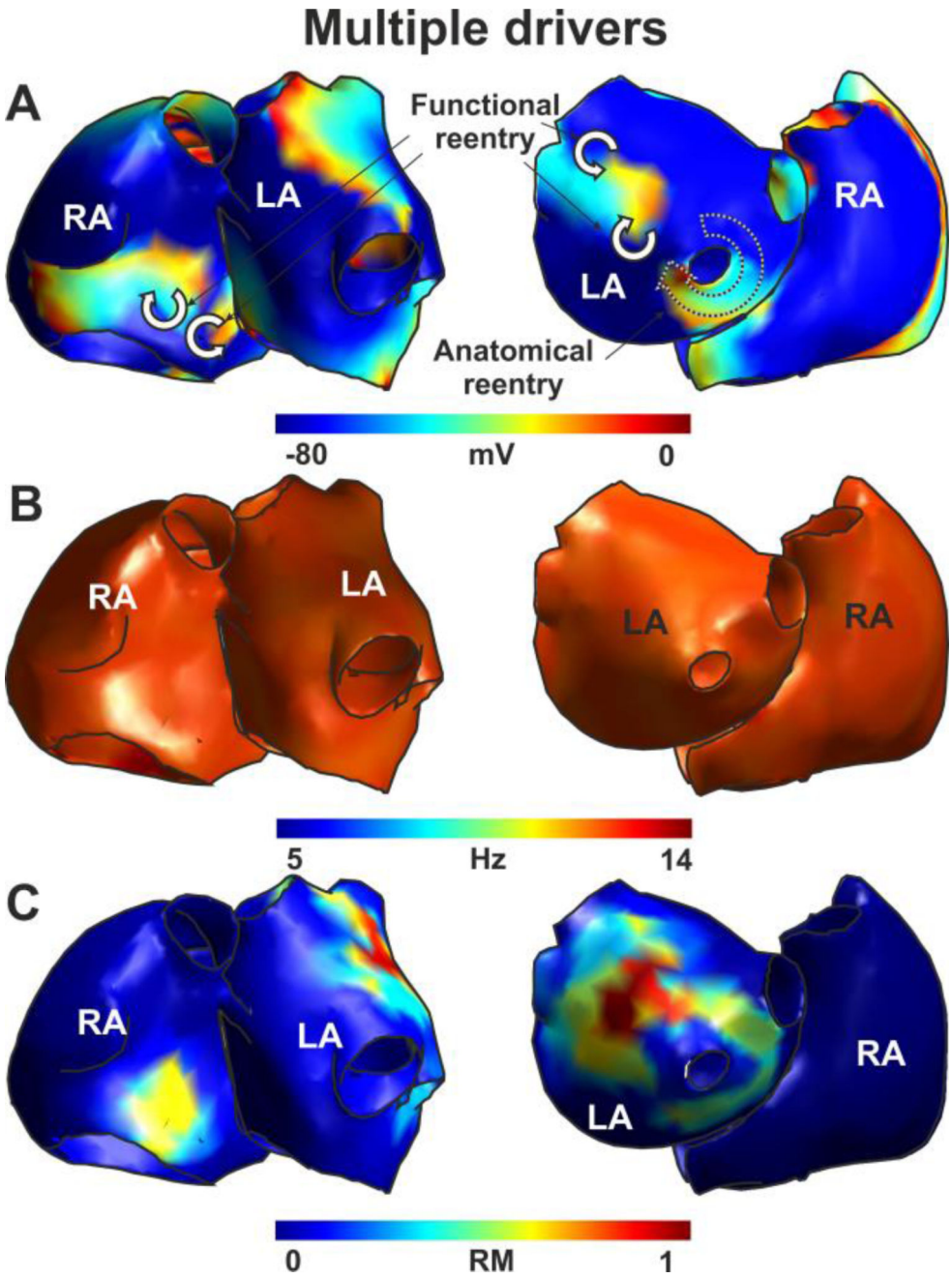

Figure 3.
Anterior and posterior views of atrial model with multiple drivers. (A) Transmembrane potentials. (B) DF map. (C) Recurrence map.

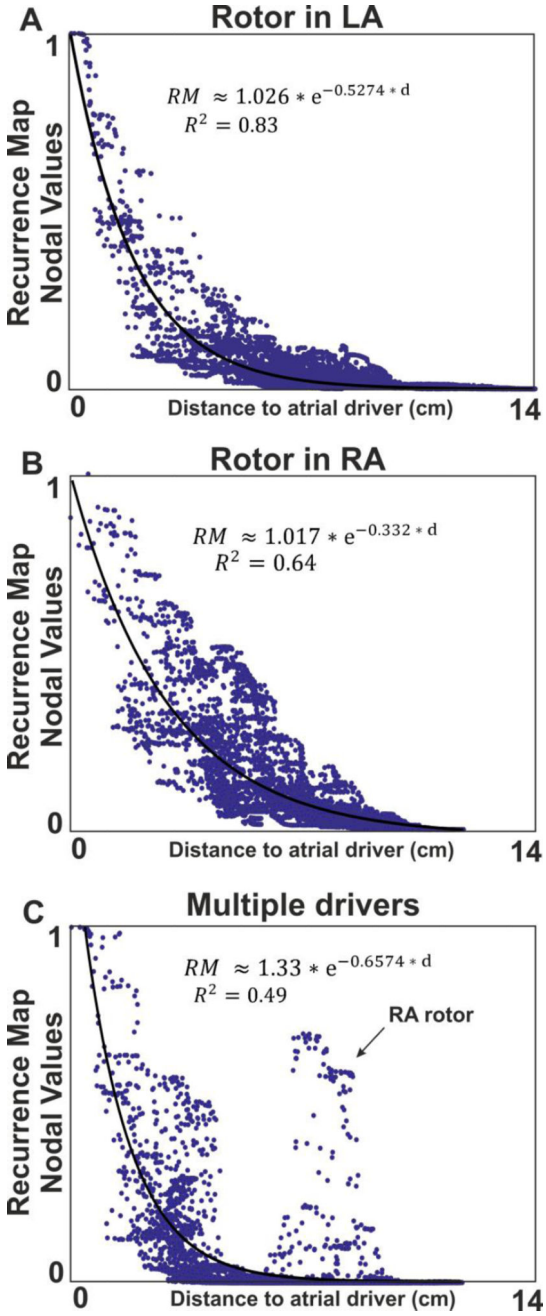

Figure 4.

Comparison between the RM values and the distance to the atrial driver for three simulations: (A) Rotor in LA without DF gradient; (B) double rotor in RA; and (C) multiple drivers. Blue dots represent the RM values obtained from the model and the black line represents the best exponential decay model fitted for these points.